NIH Public Access
Author Manuscript

The immunodominant CD8+ T cell epitope region of Theiler's virus in resistant C57BL/6 mice is critical for anti-viral immune responses, viral persistence, and binding to the host cells.

Jinjong Myoung, **Wanqiu Hou**, **Bongsu Kang**, **Michael A. Lyman**[†], **Jeong-Ah Kang**[‡], and **Byung S. Kim**[*]
Department of Microbiology-Immunology, Northwestern University Medical School, Chicago, Illinois 60611

Abstract

Theiler's virus infection induces an immune-mediated demyelinating disease, providing a relevant animal model of human multiple sclerosis. $VP2_{121-130}$-specific CD8+ T cells in resistant $H-2^b$ mice account for the majority of CNS-infiltrating CD8+ T cells. To further study the role of the CD8+ T cells, we generated a panel of mutant viruses substituted with L, G, or T at the anchor residue (M130) of the $VP2_{121-130}$ epitope. M130L virus (M130L-V) with a substitution of M with L displayed similar properties as wild-type virus (WT-V). However, M130G-V and M130T-V could not establish a persistent infection in the CNS. The level of both virus-specific CD8+ and CD4+ T cell responses is significantly reduced in mice infected with these variant viruses. While all mutant and wild-type viruses replicate comparably in BHK cells, replication of M130G-V and M130T-V in macrophages was significantly lower compared to those infected with WT-V and M130L-V. Interestingly, these mutant viruses deficient in replication in primary mouse cells showed drastically reduced binding ability to the cells. These results suggest that the anchor residue of the predominant CD8+ T cell epitope of TMEV in resistant mice is critical for the virus to infect target cells and this deficiency may result in poor viral persistence leading to correspondingly low T cell responses in the periphery and CNS. Thus, selection of the cellular binding region of the virus as the predominant epitope for CD8+ T cells in resistant mice may provide a distinct advantage in controlling viral persistence by preventing escape mutations.

Keywords

TMEV; CD8+ T cells; Epitope; Mutant viruses; CNS

INTRODUCTION

Theiler's murine encephalomyelitis virus (TMEV), an unenveloped single-stranded positive-sense RNA virus, belongs to a genus of family *Picornaviridae*. TMEV-induced demyelinating disease (TMEV-IDD) provides an excellent infectious animal model for human multiple sclerosis, as these diseases show many similarities, among which are immune-mediated

[*] All correspondence should be made to Dr. Byung S. Kim, Department of Microbiology-Immunology, Northwestern University Medical School, 303 East Chicago Ave., Chicago, IL 60611. E-mail: bskim@northwestern.edu; Tel. (312) 503-8693; Fax. (312) 503-1339.
[†]Present Address: Gemini Science, Inc., San Diego, CA 92121
[‡]Present Address: Department of Pediatrics, University of Chicago Medical School, Chicago, IL 60637

destruction of myelin sheath and gender-biased susceptibility (Kim et al., 2000). The exact mechanism of immune-mediated pathology in TMEV-IDD remains elusive. A wealth of evidence, however, supports the hypothesis that cytokine release by TMEV-specific Th1 cells leads to the recruitment and activation of macrophages within the CNS of susceptible mouse strains. Not only as effectors of demyelination (Liuzzi, Riccio, and Dal Canto, 1995;Rossi et al., 1997) but also as regulators of initial Th1/Th2 differentiation (Palma et al., 2002) in TMEV infection, macrophages are considered to be a determining factor for persistent infection (Lipton, Kumar, and Trottier, 2005).

Virus-specific CD8$^+$ T cells are critical in resolving viral infection by killing virus-infected host cells. Perforin- (Palma et al., 2001) or β2 microglobin-deficient (Pullen et al., 1993) mice with resistant H-2^b background developed demyelination and a low but significant level of clinical diseases. An immunodominant epitope recognized by >70% CNS-infiltrating CD8$^+$ T cells and 2 minor epitopes (<10%) were identified from TMEV-infected C57BL/6 mice (Dethlefs et al., 1997;Johnson et al., 1999;Lyman et al., 2002). C57BL/6 mice tolerized in the CD8$^+$ T cell response to the major epitope by either infusion of soluble epitope peptide or in transgenic mice expressing the epitope-bearing viral protein become susceptible to TMEV-induced demyelination (Mendez-Fernandez et al., 2003). Thus, CD8$^+$ T cell response to the predominant epitope appears to be critical in maintaining resistance. Although TMEV-specific CD8$^+$ T cell responses seem to be important in viral resolution, their role in the pathogenesis/protection in TMEV-IDD remains controversial (Fuller et al., 2005). A group of investigators have proposed that cytotoxic CD8$^+$ T cell response is necessary for clinical manifestation as well (Rivera-Quinones et al., 1998), based on observation that the lack of clinical disease in perforin-deficient mice with apparent demyelination (Murray et al., 1998). Furthermore, CD4$^+$ T cells may also play a protective role in resistant C57BL/6 mice. MHC class II-deficient mice are susceptible to TMEV-induced demyelination and ultimately clinical signs, such as spasticity and paralysis (Njenga et al., 1996). In addition, antibody-deficient μMT mice in the absence of CD8$^+$ T cells are also susceptible to TMEV-induced encephalitis although the deficiency in CD8$^+$ T cells alone is not sufficient to induce clinical outcome (Kang et al., 2005).

Thus, identification of the potential role of CD8$^+$ T cells specific for the predominant TMEV epitope is critically important in understanding the mechanisms of the protection and/or pathogenesis of TMEV. In addition, understanding the compensatory role of CD8$^+$ T cells recognizing minor epitopes in the absence of T cells recognizing the predominant epitope is equally important. Furthermore, a variety of viruses, such as HIV (Allen et al., 2005;Goulder and Watkins, 2004) and LCMV (Pircher et al., 1990;Velloso et al., 2004), evade potent cytotoxic T cells by accumulating spontaneous mutations in the epitope regions. However, no CTL escape mutant from TMEV-infected animals has been reported so far (Brahic, Bureau, and Michiels, 2005). To address some of these questions, we constructed a series of '*in vitro* generated' CTL escape mutant viruses by single amino acid substitutions at residue 130 of the predominant VP2 epitope. Our results in this study clearly demonstrate that mutant viruses (M130G-V and M130T-V) substituted with residues with low reactivity to CD8$^+$ T cells could not establish persistent infection in the CNS, despite their comparable replication to WT- and M130L-V in BHK-21 cells. The levels of both VP2$_{121-130}$-specific CD8$^+$ T cells and virus-specific CD4$^+$ T cells in the CNS were significantly reduced in mice infected with these mutant viruses in contrast to those in mice infected with WT-V or M130L-V. Interestingly, such drastic reduction in CD8$^+$ T cell response to VP2$_{121-130}$ was not accompanied by a compensatory increase of other epitope-specific CD8$^+$ T cells. This unexpectedly low T cell response and viral persistence apparently resulted from the inability of the mutant viruses to bind their cellular receptors. These results strongly suggest that the TMEV VP2$_{121-130}$ CD8$^+$ T cell epitope region is critical for viral infection of target cells. The necessity of the intact epitope

region for viral binding to the target cells may limit emergence of CTL escape mutants in this region.

RESULTS

Hydrophobicity and size of the amino acid residue at the position VP2$_{130}$ affect binding of VP2$_{121-130}$ peptide to H-2D^b molecule

The VP2 130M residue is believed to be an anchor residue of the predominant H-2D^b-restricted VP2$_{121-130}$ epitope. To study the role of CD8$^+$ T cells in C57BL/6 mice, we substituted the VP2$_{130}$ methionine (M) residue with 17 different amino acids, excluding P and C which result in drastic structural changes. (Figure 1A). It was previously shown that incubation of RMA-S cells with MHC class I-binding peptides has shown to enhance surface expression of the MHC class I molecules on these cells by stabilizing the peptide-MHC complex (Ljunggren et al., 1990). As expected, the peptides substituted with consensus anchor residues (I and L) stabilized comparable levels of surface D^b expression (Figure 1B). Interestingly, surface MHC class I molecules were also stabilized by peptides substituted with some other hydrophobic non-consensus amino acids, such as A, F, and V, while none of polar amino acid substitutions yielded such stabilization. In addition to hydrophobicity, the size of amino acid also seems to play a role, as small G and large W which are both hydrophobic could not stabilize surface expression. Stabilization of surface K^b expression by the analog peptides was also analyzed. However, no significant stabilization was observed by any of the peptides utilized, indicating that these peptides do not bind K^b molecules (data not shown).

Binding affinity of peptides to D^b molecules affects immunological reactivity by CD8$^+$ T cells

To correlate the binding ability of H-2D^b to peptides with specific CD8$^+$ T cell activation, we re-stimulated freshly isolated CNS-infiltrating MNC from mice at 8 days post TMEV-infection with a panel of substituted peptides and examined their ability to stimulate intracellular and extracellular interferon-γ production, as well as target cell lysis (Figure 1C). All the peptides with high binding affinity, i.e. native (130M) and substituted with A, F, I, L, and V, induced higher levels of IFN-γ production. In addition, these peptides induced more effective lysis of EL-4 cells loaded with the peptides. These results indicate that substituted peptides with high affinity to MHC I molecules display strong activation of epitope-specific CD8$^+$ T cells. However, peptides with low affinity induce varying patterns of immunological reactivity in CD8$^+$ T cells. The affinity of a peptide for D^b correlates well with its ability to induce IFN-γ production and target cell lysis by CD8$^+$ T cells, e.g. poor D^b-binding peptides substituted with N, Q, R, or S could neither up-regulate IFN-γ production in CD8$^+$ T cells nor lead to lysis of target cells (Figure 1C). Peptides substituted with 130G, K, H, or Y induced lower but significant levels of IFN-γ production. However, the level of IFN-γ production by the peptides did not correspond to their ability to lyse the target cells (e.g. high lysis of target cells loaded with 130K and Y peptides, but low lysis with 130G and H). These data suggest that low-affinity peptides are unable to stably bind to class I molecules which is required to transmit activation signals through TCR complex on CD8$^+$ T cells for IFN-γ production. However, some such weak interactions may be sufficient for cytolytic function. It is also interesting to note that intracellular IFN-γ expression did not always correlate with the number of IFN-γsecreting CD8$^+$ T cells. The differences, particularly by intermediate inducers (130E, N and R), may reflect that secretion of IFN-γ requires stronger stimulatory signal than intracellular cytokine expression (Horton et al., 2004).

Wild-type and mutant viruses, containing a single amino acid substitution at VP2-130(M) with L, T, or G replicate similarly in BHK cells

To investigate the effect of a single amino acid substitution at the anchor position VP2$_{130}$ on induction of virus-specific T cell responses *in vivo*, we generated several mutant viruses by

site-directed mutagenesis at the position as described in Figure 2A. The amino acids to be substituted were selected based on the affinity of each altered peptide for D^b and its reactivity to epitope-specific $CD8^+$ T cells (Figure 1). These include substitution with L, which is one of the consensus D^b motifs retaining strong affinity to D^b and vigorously stimulating $CD8^+$ T cells, substitutions with G and T, inducing intermediate levels of IFN-γ production and low cytotoxic activity, and substitution with S, evoking only marginal level of $CD8^+$ T cell stimulation. As a positive control, WT-virus created from the same expression vector of TMEV BeAn strain (pSBW) was included (Figure 2A). All the viruses used, except M130S-V, demonstrate comparable growth in BHK cells (Figure 2B). However, M130S-V showed a significant growth deficiency by one order of magnitude at 14 hours post-infection and thereafter. Therefore, M130S-V was not included in subsequent studies.

Viral replication in BHK cells does not correlate with *in vivo* viral persistence and peripheral immune responses

To examine viral replication *in vivo*, viral titres were measured in the brains and spinal cords of mice infected with 3×10^6 pfu of each virus. At 8 days post-infection, the level of viral titers in M130L-V-infected mice was comparable to that of WT-V-infected mice. However, M130T-V and M130G-V showed 10-fold and 10,000-fold lower viral titers in the CNS respectively compared to WT-V (Figure 3A). At 21 days post infection, however, no detectable viral titers from any of the virus-infected mice were observed in 3 repeated experiments. Since it has previously shown with CVB3, another picornavirus that some replicating viral genomes failed to produce lytic plaques on infected cells (Feuer et al., 2002;Kim et al., 2005), the viral message levels in the CNS were further assessed. Analysis of viral message levels in these mice using real-time PCR indicated that viral message levels at 8 days post-infection are closely correlated with the levels of viral replication determined by plaque assay (Figure 3A). As expected, the viral message levels at 21 days post infection were low although the levels of M130L-V and M130G-V were higher than that of WT-V. Nevertheless, the variant viruses appeared to be replicated at a low level in the CNS. The low or undetectable level of TMEV messages in the CNS of C57BL/6 mice after 21 d post infection was consistent with the previous report (Lipton, Kumar, and Trottier, 2005). This may reflect the balances between the reduced levels of virus-specific $CD8^+$ T cells and viral infectivity of the variant viruses to the host cells. Nevertheless, such differences do not appear to be strong enough to alter the pathogenic property of the viruses.

As TMEV-specific antibody responses were previously shown to be involved in resistance to viral infection and low viral persistence in C57BL/6 mice (Kang et al., 2005), the level of virus-specific IgG responses in the serum was analyzed. As shown in Figure 3B, significantly lower antibody responses were induced in M130G-V and M130T-V-infected mice compared to those from mice infected with either WT or M130L-V ($p<0.05$ at all dilution points). Therefore, the virus-specific antibody response does not appear to be responsible for early viral clearance from the CNS. To test whether higher peripheral T cell responses in M130G/T-V-infected mice are responsible for early viral clearance, splenic $CD4^+$ and $CD8^+$ T cell responses to viral epitopes were assessed by ELISPOT assay (Figure 3C). The level of IFN-γ-secreting virus-specific $CD4^+$ T cells was not affected in any of the experimental groups, while that of $CD8^+$ T cells was greatly reduced in M130G/T-V-infected mice compared to M130L-V or WT-V-infected animals ($p<0.005$). Therefore, peripheral immune responses to the virus do not seem to be responsible for the unusually rapid clearance of M130G-V and M130T-V.

M130G-V and M130T-V are unable to induce CNS-infiltrating $CD8^+$ T cell responses to either native or altered epitopes

Although infection with M130G/T-V did not induce peripheral $CD8^+$ T cells specific for the native epitope ($VP2_{121-130M}$), such $CD8^+$ T cells may be detectable in the CNS, the site of

viral persistence. In addition, it is equally possible that these mutant viruses may induce CD8^{+} T cells preferentially reactive to their own altered epitopes. To test this possibility, we assessed the epitope reactivity of CD8^{+} T cells in the CNS of mice by intracellular IFN-γ-production following stimulation with the native epitope peptide and altered peptides (Figure 4). WT-V-infected mice resulted in 53% of CNS-infiltrating CD8^{+} T cells reactive to the native 130M, 20% to 130L, 7% to 130G and 4% to 130T (Figure 4A). M130L-V containing a consensus binding residue for D^b induced a significant level of CD8^{+} T cells reactive to 130M (41%) and 130L (31%). Thus, it appears that as much as 75% of $VP2_{121-130}$(130M)-reactive CD8^{+} T cells recognized 130L peptide in M130L-V-infected animals, while only 37% of 130M-specific CD8^{+} T cells are 130L-reactive in WT-V infected mice, suggesting that M130L-V infection preferentially induce CD8^{+} T cells favoring reactivity to 130L within the T cell repertoire reactive to 130M. However, M130L-V failed to induce a higher level of CD8^{+} T cells reactive to the altered epitope compared to the native epitope. In addition, M130G-V and M130T-V failed to induce vigorous CD8^{+} T cell responses to either the native 130M or their own substituted epitopes, 130G and 130T, respectively ($p<0.001$). Furthermore, there was no significant compensatory increase in the CD8^{+} T cell population specific for minor epitopes to balance the reduced level of CD8^{+} T cells specific for the predominant epitope (Figure 4B). Thus, the reduction of CD8^{+} T cells reactive to the epitope region appears to reflect inability of the variant viruses to induce CD8^{+} T cell responses (Figure 4C). In order to examine further the possibility that these infected mice may induce comparable level of specific CD8^{+} T cells which do not produce IFN-γ, the presence of epitope-specific CD8^{+} T cells in the CNS was assessed using D^b-130M (WT) tetramer (Figure 4D). Similar levels of CD8^{+} T cells reacted with the tetramer compared to the intracellular IFN-γ production. Therefore, it is most likely that M130G/T-V fail to induce cognate CD8^{+} T cell responses to this epitope region in infected animals.

Both M130G-V and M130T-V induce weak virus-specific CD4^{+} T cell responses in the CNS

Since the low levels of virus-specific CD8^{+} T cell and antibody responses paralleled the inability of M130G/T-V to persist *in vivo*, we next sought to assess the level of epitope-specific CD4^{+} T cells, which were shown to be important in virus clearance in C57BL/6 mice (Njenga et al., 1996). The levels of CD4^{+} T cell responses to two representative immunodominant epitopes, $VP2_{206-220}$ and $VP4_{25-38}$ were assessed by intracellular IFN-γ production (Figure 5) as shown previously (Kang, Kang, and Kim, 2005). Like CD8^{+} T cell responses, the proportion ($p<0.05$) and the number ($p<0.001$) of epitope-specific CNS CD4^{+} T cells induced following infection with M130G/T-V were significantly lower at 8 d post-infection compared to that induced by WT-V and M130L-V (Figure 5). In addition, the overall CD4^{+} T cell infiltration to the CNS was also significantly reduced following infection with these mutant viruses. Therefore, as seen for the antibody and CD8^{+} T cell responses, these variant viruses except M130L-V, are unable to induce strong TMEV-specific CD4^{+} T cell responses.

M130G/T-V viruses show replication deficiency in primary macrophages

It is conceivable that M130G/T-V may not be able to replicate to the extent of WT-V and M130L-V in mouse cells, resulting in the lack of viral expansion/replication and poor induction of immune responses. To explore this possibility, the replication levels of wild-type and mutant viruses in thioglycollate-induced peritoneal exudate macrophages were assessed (Figure 6A), as this cell type is known to be the main reservoir of TMEV (Clatch et al., 1990;Rossi et al., 1997). The level of M130G/T-V replication in macrophages was significantly lower ($p<0.05$ for M130G-V, $p<0.005$ for M130T-V) compared to that of WT-V or M130L-V. Therefore, the lack of viral persistence in the CNS of mice infected with these mutant viruses may reflect the deficient replication in mouse host cells. To further test whether this low viral replication in macrophages is due to the inability of M130G/T-V to bind to the cells, we determined the ability of theses viruses to bind macrophages. Interestingly, both M130G-V and M130T-V

bind macrophages far less well compared to WT-V. M130L-V, which shows viral replication similar to WT-V, binds the macrophages better than M130G/T-V, but less well compared to WT-V (Figure 6B). The differences in the replication levels of M130G-V and M130T-V despite a comparable level of macrophage binding suggest a potential involvement of post-attachment steps. Therefore, viral binding above a certain threshold by M130L-V may be sufficient for comparable viral replication. Similar binding deficiencies of the mutant viruses were observed with bone-marrow-derived DC (Figure 6C). The deficiencies in DC-binding by these viruses may also negatively affect the ability to induce strong T cell responses specific for viral determinants, in particular CD8$^+$ T cell responses.

DISCUSSION

The importance of CD8$^+$ T cells in conferring resistance to TMEV infection has been extensively studied not only by employing various mice deficient in immune related genes (Begolka et al., 2001;Palma et al., 2001;Pullen et al., 1993) or transgenic expression of H-2D^b (Lin et al., 2002), but also by enumerating virus-specific CD8$^+$ T cells in the CNS of differentially susceptible mice (Kang, Lyman, and Kim, 2002b;Lyman et al., 2004). One immunodominant CD8$^+$ T cell epitope (VP2$_{121-130}$) was identified (Johnson et al., 1999) and shown to be critical for maintaining resistance in genetically resistant C57BL/6 mice (Lyman et al., 2004;Mendez-Fernandez et al., 2003). However, the involvement of CD8$^+$ T cells in the pathogenesis of clinical disease remains to be elusive (Fuller et al., 2005;Murray et al., 1998;Rivera-Quinones et al., 1998). To study further the role of epitope-specific CD8$^+$ T cells in TMEV-IDD, we have first analyzed a panel of the epitope peptides, containing single amino acid substitutions at position VP2$_{130}$ (M130) for their ability to interact with class I molecules and stimulate specific CD8$^+$ T cells. Interestingly, some apparent non-binders were able to result in cytolytic activity and/or IFN-γ production (Figure 1). It has also previously been shown that some MHC class I-binding peptides failed to induce CTL with effector functions such as target cell lysis or cytokine expression (Feltkamp et al., 1994;Lyman et al., 2002). The discrepancies between binding and stimulatory function of the peptides may reflect the insensitivity of the MHC-binding assay (Feltkamp et al., 1995) and the involvement of different CD8$^+$ T cell subpopulations and/or stimulatory signal requirements (Andersen et al., 2000). Altered epitope peptides (130F/I/L) with high MHC-binding affinity stimulated specific CD8$^+$ T cells to produce high level of IFN-γ (Figure 1). Likewise, peptides (130K/W/H) with low affinity for MHC class I molecules generally induced low level of IFN-γ.

Based on the above binding and stimulation studies with altered peptides, we generated variant TMEV carrying the altered epitope region by introducing non-charged polar or charged amino acid substitutions at the position of VP2$_{130}$. Intriguingly, none of charged amino acid substitutions (e.g. D, E, K, etc) produced viable viruses (data not shown), indicating the importance of the hydrophobic nature of this anchor residue for viral replication. In contrast, TMEV (M130G-V and M130T-V) substituted with non-charged polar amino acid (G and T, respectively) at the position were able to replicate comparably to the wildtype virus or virus with L substitution (M130L-V) in BHK 21 cells (Figure 2B). Therefore, some of these substitutions appear to be well tolerated for viral replication in BHK cells. In contrast, these mutant viruses (M130G/T-V) showed significantly lower replication ($p<0.05$ and $p<0.001$, respectively) compared to WT-V in primary macrophages (Figure 6A), suggesting that the replication/infection of these mutant viruses is severely compromised in mouse primary cells. Further studies demonstrated that the poor replication of these mutant viruses appears to reflect their inefficient binding to the cells in general (Figure 6B). As macrophages are known to be a major viral reservoir, antigen presenting cells, as well as one of the main effectors of demyelination, the inability of mutant viruses to establish infection in this cell type is likely to result in inferior viral persistence and virus-specific immune responses *in vivo*. This binding deficiency is not limited to macrophages as these variant viruses showed similar binding

reductions to DC although the degree may be slightly different depending on the cell types (Figure 6C). Therefore, these viruses are most likely defective in infection of many different host cell types differentially, which may result in some discrepancies between the levels of viral persistence in the CNS (Figure 3) and in vitro assays for binding and replication (Figure 6). In addition, DC are known to be the most important APC in T cell responses to virus in the periphery and the CNS (Granucci, Foti, and Ricciardi-Castagnoli, 2005;Greter et al., 2005;McMahon et al., 2005). Thus, the reduced levels of virus binding/infection to DC may also contribute to the poor T cell responses to the mutant viruses. Since the precise correlation of CNS viral persistence to one factor alone is not observed, all of these and perhaps additional unknown factors may collectively influence the level of viral persistence in vivo.

It has previously been reported that BeAn and DA strains of TMEV use sialic acid as co-receptors for cell entry (Shah and Lipton, 2002;Zhou et al., 1997;Zhou et al., 2000). The residues known to be involved in interaction of TMEV with sialic acid moiety are located in close proximity to VP2-M130, suggesting that alteration of M130 may influence on receptor binding (Supplemental Figure 1). However, it is unlikely that this residue is directly involved in interacting with sialic acid since M130G/T-V are capable of infecting/replicating in BHK cells comparably to WT viruses (Figure 2). In addition, the $VP2_{130}$ residue is located in one of β-sheets of the VP2 chain and not in the loops containing residues interacting with the sugar moiety (Supplemental Figure 1A). Furthermore, this residue is not exposed on the surface of the TMEV protomer required for potential interaction with sialic acid (Supplemental Figure 1B). However, it is conceivable that substitution of M with G or T at the position might induce a more global change on virion structure such that M130G/T-V display compromised interactions with cellular receptor(s) and/or co-receptors, including sialic acid residues. Nevertheless, these viruses appear to retain reduced but some ability to infect macrophages. Certain variant TMEV similarly substituted at the position $VP2_{125}$ within the predominant epitope region (e.g. S125G-V) also resulted in poor binding to macrophages, deficiencies in viral persistence and $CD8^+$ T cell response in the CNS (Supplemental Figure 2). Therefore, not only the M130 residue but also adjacent residues may display similar effects. These results support the importance of this epitope region in the binding to the host cells for resistant C57BL/6 mice. Selection of the cellular binding region of the virus as the predominant epitope for $CD8^+$ T cells may have a distinct advantage in controlling viral persistence, as an establishment of escape mutant viruses in resistant $H-2^b$ mice would be extremely difficult without compromising the infectivity. In fact, no naturally occurring CTL escape mutants at this region have been reported.

It is interesting to note that in resistant C57BL/6 ($H-2^b$) mice, 50–70% of infiltrating $CD8^+$ T cells are $VP2_{121-130}$-specific and are critical for viral clearance (Lyman et al., 2004;Mendez-Fernandez et al., 2003). Despite the predominance of this single $CD8^+$ T cell epitope throughout the infection, we have not been able to isolate escape mutants, and none have been reported as of yet. It is also intriguing to note that the $CD8^+$ T cell response induced by a mutant virus (e.g. M130L-V), even with similar levels of viral persistence and immune responses, preferentially react with the native epitope, M130 rather than their own mutated epitopes such as M130L. Our results in this study demonstrate that viruses with non-conservative amino acid substitutions at $VP2_{130}$ are compromised in binding to cellular receptors on primary cells from C57BL/6 mice, leading to reduced viral persistence *in vivo*. Therefore, the lack of emergence of mutant viruses at the epitope region may reflect the importance of this region in maintaining viral persistence and/or in determining host range and tissue tropism. Our observation is consistent with the recent suggestion by Brahic and colleagues that "a high fitness cost" may be required for mutation in this epitope since it is conserved by all Theiler's virus strains despite the selection pressure of $CD8^+$ T cells (Brahic, Bureau, and Michiels, 2005). Interestingly but not surprisingly, these mutant viruses also displayed poor binding to macrophages derived from $H-2^s$-bearing SJL/J mice (data not shown). These preliminary results suggest that this

region might be involved in virus binding regardless of their MHC haplotype. Further crystallographic structural studies with the mutant viruses may reveal the potential alterations in the putative cellular receptor binding-region of the virus. In addition, these variant viruses may also provide an important tool in identifying cellular receptor(s) for TMEV infection.

MATERIALS AND METHODS

Animals

Female C57BL/6 mice from the Charles River Laboratories (Charles River, MA) through the National Cancer Institute (Frederick, MD) were housed in the Animal Care Facility of Northwestern University. Animal experiments were conducted according to the protocols approved by Northwestern university animal care and use committee.

Cell lines

The EL-4 (H-2D^b) and BHK-21cell lines were obtained from American Type culture collection (Bethesda, MD) and was maintained in RPMI 1640 supplemented with 5% FBS. RMA-S cell line was obtained from Dr. Jeffrey Bluestone (University of California, San Francisco) with permission from Dr. Klas Karre (Karolinska Institute, Stockholm, Sweden).

Synthetic peptides and antibodies

All peptides used were synthesized with the rapid multiple peptide synthesis system (RaMPS; Dupont Co., Wilmington, DE) and used as described previously (Kang, Lyman, and Kim, 2002b). All antibodies used were purchased from BD Pharmingen.

Virus preparation and infection

Viruses used in this study were generated, propagated, and titred in BHK-21 cells grown in Dulbecco's modified Eagle medium supplemented with 7.5% donor calf serum. For intracerebral (i.c.) infection, 30 μl virus solution, containing 3×10^6 pfu, was injected into the right cerebral hemisphere of 6–8 week-old mice anesthetized with isoflurane.

Site-directed mutagenesis and mutant virus generation

A full-length expression clone pSB3 (Pevear et al., 1987) was modified to reflect the nucleotide sequence of our highly pathogenic BeAn S2 stock. The regions of pSB3 differing in the sequence of BeAn S2 (Genbank Accession number # DQ401688) were replaced with those of S2. In addition, 12 nucleotides between T7 promoter and 5′ untranslated region of the TMEV genome were deleted and TT were added immediately after T7 promoter. Plasmid constructs for mutant viruses, harboring a single amino acid substitution in the predominant CD8$^+$ T cell epitope in C57BL/6, were generated using QuikChange® II XL Site-directed Mutagenesis Kit (Stratagene, Cedar Creek, TX). A mutation was introduced into an expression cDNA clone (pSBW) of TMEV BeAn strain (Accession number # DQ401688) according to the manufacturer's instruction. Briefly, two complementary mutagenic oligonucleotides were designed so that those oligonucleotides bind to pSBW except the target site. Mutant viral DNA was amplified with pfu Turbo® (Stratagene, Cedar Creek, TX) based on polymerase chain reaction. Parental strands were destroyed by Dpn I with the digestion mixture and subsequently used to transform JM109 *E. coli* competent cells. Sequences were verified at the Sequencing Core Facility of Northwestern University. Viral RNA was then transcribed *in vitro* from wild-type or mutated pSBW using T7 RNA polymerase in the presence of RNasin, an RNase inhibitor (Promega, Madison, WI). The integrity and size of viral RNA was verified on 1.2% agarose gel. Each viral RNA was transfected into BHK cells using Lipofectamine 2000® (Invitrogen, Carlsbad, CA). Cytopathic effect was observed from 3 days post-transfection.

Viruses were harvested 5–7 days after transfection and re-infected into BHK cells to further amplify viruses.

Viral replication assay

Wild-type or mutant virus was infected at MOI 10 into BHK cells with rocking and resting for 1 hour followed by extensive wash. Cells were then cultured for various time periods at 33° C. Both cells and supernatants were harvested and kept at −70° C until use. To obtain macrophages, thioglycollate (1 ml of 3%) medium (Difco, Detroit, MI) was injected into peritoneal cavity of C57BL/6 mice and peritoneal exudate cells were collected 3 days later. Cells (2×10^6) were washed and then seeded into a 24-well plate for 2 hours at 37° C. After removal of non-adherent cells, the remaining adherent cells were used for viral infection study. Wild-type and mutant viruses were infected at MOI 10 at room temperature for 1 h, unbound viruses were removed, and then further cultured in 1ml of RPMI 1640 medium. After 24 hours, culture supernatants were used to determine the level of productive viral replication by plaque assay on BHK monolayers (Fuller et al., 2005).

Semi-quantitative real-time PCR

Total RNA was isolated from tissue homogenates using Trizol® Reagent (Invitrogen, Carlsbad, CA), and resuspended in 0.1% DEPC water containing RNasin® (Promega, Madison, WI). cDNA was synthesized by utilizing SuperScript™ III Reverse Transcriptase (Invitrogen, Carlsbad, CA) and oligo dT primers and then amplified using the Bio-Rad iCycler iQ system (Bio-Rad Laboratories, Hercules, CA). Real-time PCR (40 cycles) was carried out using iQ SYBR Green supermix (Bio-Rad Laboratories) with the following sequence specific primers. GAPDH: 5′-AACTTTGGCATTGTGGAAGG-3′ and 5′-ACACATTGGGG-GTAGGAACA-3′; TMEV: 5′-CTGCAATTGGAACTGACCCAGATG-3′ and 5′-ATGTCGTGA-CACAGCCAGAGAT-3′

Isolation of CNS-infiltrating mononuclear cells (MNC)

Mice were perfused with 40 ml of sterile Hank's balanced salt solution (HBSS) and excised brains and spinal cords were homogenated. CNS-infiltrating MNC were then enriched in the 1/3 bottom fraction of a continuous Percoll (Pharmacia, Piscataway, NJ) gradient after centrifugation for 30 min at 27,000g as described previously (Fuller et al., 2005).

Peptide binding assay on RMA-S cells

For H-2D^b binding assays, RMA-S cells were loaded with various peptides at final 40 μM for 16–18 hours at 37° C as described previously (Lyman et al., 2002). Levels of surface MHC class I molecule expression were assessed by flow cytometric analysis using FITC-conjugated mouse monoclonal antibodies specific for H-2D^b (Clone CTDb; Cedarlane Laboratories Ltd., Ontario, Canada) or H-2K^b (Clone CTKb; Cedarlane Laboratories).

Intracellular staining of cytokine production

Freshly isolated CNS-infiltrating MNC were cultured in 96-well round bottom plates in the presence of relevant or control peptide as described previously (Lyman et al., 2004). Allophycocyanin-conjugated anti-CD8 (clone Ly2) or anti-CD4 (clone L3T4) antibody and PE-labeled rat monoclonal anti-IFN-γ (XMG1.2) antibody were used for intracellular cytokine staining. Cells were analyzed on a Becton Dickinson FACS Calibur or FACS Sort flow cytometer. Live cells were gated based on light scatter properties.

IFN-γ ELISPOT assay and antibody ELISA

The number of antigen-specific IFN-γ-secreting CD8$^+$ T cells (2×10^4 CNS-infiltrating MNC) was enumerated by ELISPOT assay after 18 hr of *ex vivo* stimulation with various peptides at final 2 μM with 1×10^6 irradiated splenic cells. Plates were further incubated with biotin-conjugated anti-IFN-γ antibody (Endogen, Rockford, IL), followed with streptavidin-HRP and then developed using 3-amino-9-ethyl-carbazole (Sigma-Aldrich, St. Louis, MO) as described previously (Kang, Lyman, and Kim, 2002a). Antibody response was examined using UV-TMEV-coated plates by ELISA starting with 1/100-diluted serum samples from infected animals as described elsewhere (Kang, Lyman, and Kim, 2002a).

CTL assay

EL-4 cells were loaded with WT or mutant peptides and used as target cells to analyze induction of each peptide-reactive CD8$^+$ T cells in the CNS using a standard ^{51}Cr-release assay as described previously (Lyman et al., 2002). After extensive wash, peptide-loaded ^{51}Cr-EL-4 target cells (3×10^3) were added to varying numbers of fresh CNS effector cells followed by incubation at 37°C for 6 hours. Supernatants were collected and the mean radioactivity values were calculated from duplicate wells. Percentage of specific lysis was computed according to the formula: ((experimental ^{51}Cr release – spontaneous ^{51}Cr release)/(maximum ^{51}Cr release with 1% Triton X-100 – spontaneous ^{51}Cr release)) × 100%. Spontaneous lysis was less than 15% throughout the assays.

Generation of bone marrow-derived dendritic cells (BM DC)

BM cells harvested from femurs and tibias of C57BL/6 mice were cultured in 24-well plates (Corning Coster, Cambridge, MA) ($2x10^6$/well) in 1 ml culture medium supplemented with 20 ng/ml murine rGM-CSF (Peprotech, Rocky Hill, NJ). The selection procedures were similar to those reported initially by Inaba et al. (Inaba et al., 1992) with minor modifications as described (Hou et al., 2003). On day 5, DC were harvested, washed twice and used in subsequent experiments.

Virus-cell binding assay

Single-cell suspensions of BM DC or peritoneal exudate cells (PEC) were incubated for 1 h at 4°C with TMEV BeAn (MOI = 100), washed extensively with ice-cold PBS, and fixed in 1% paraformaldehyde as described by Mena et al. (Mena, Roussarie, and Brahic, 2004). Fixed cells were washed with PBS, blocked with normal goat serum and then reacted with the 8C monoclonal Ab to the TMEV capsid protein (Crane et al., 1990) followed by FITC-conjugated goat F(ab′)$_2$ anti-mouse immunoglobulin (BioSource International, Camarillo, CA). Labeled cells were analyzed on a FACS Calibur flow cytometer using the CellQuest software program. Mean log fluorescence intensity (MFI) values were obtained by subtracting the MFI of the isotype control from the MFI of the 8C monoclonal Ab stained sample.

Statistical analysis

Data are shown as mean ± SD of either 2–3 independent experiments or one representative from at least three independent experiments. The significance of differences in the mean values was determined by Student's *t* test. *p* values of < 0.05 were considered statistically significant.

Supplementary Material

Refer to Web version on PubMed Central for supplementary material.

References

Allen TM, Altfeld M, Geer SC, Kalife ET, Moore C, O'Sullivan K M, Desouza I, Feeney ME, Eldridge RL, Maier EL, Kaufmann DE, Lahaie MP, Reyor L, Tanzi G, Johnston MN, Brander C, Draenert R, Rockstroh JK, Jessen H, Rosenberg ES, Mallal SA, Walker BD. Selective escape from CD8+ T-cell responses represents a major driving force of human immunodeficiency virus type 1 (HIV-1) sequence diversity and reveals constraints on HIV-1 evolution. J Virol 2005;79:13239–49. [PubMed: 16227247]

Andersen H, Dempsey D, Chervenak R, Jennings SR. Expression of intracellular IFN-γ in HSV-1-specific CD8+ T cells identifies distinct responding subpopulations during the primary response to infection. J Immunol 2000;165:2101–7. [PubMed: 10925295]

Begolka WS, Haynes LM, Olson JK, Padilla J, Neville KL, Dal Canto M, Palma J, Kim BS, Miller SD. CD8-deficient SJL mice display enhanced susceptibility to Theiler's virus infection and increased demyelinating pathology. J Neurovirol 2001;7:409–20. [PubMed: 11582513]

Brahic M, Bureau JF, Michiels T. The genetics of the persistent infection and demyelinating disease caused by Theiler's virus. Annu Rev Microbiol 2005;59:279–98. [PubMed: 16153171]

Clatch RJ, Miller SD, Metzner R, Dal Canto MC, Lipton HL. Monocytes/macrophages isolated from the mouse central nervous system contain infectious Theiler's murine encephalomyelitis virus (TMEV). Virology 1990;176:244–54. [PubMed: 2158691]

Crane MA, Jue C, Mitchell M, Lipton H, Kim BS. Detection of restricted predominant epitopes of Theiler's murine encephalomyelitis virus capsid proteins expressed in the lambda gt11 system: differential patterns of antibody reactivity among different mouse strains. J Neuroimmunol 1990;27:173–86. [PubMed: 1692032]

Dethlefs S, Escriou N, Brahic M, van der Werf S, Larsson-Sciard EL. Theiler's virus and Mengo virus induce cross-reactive cytotoxic T lymphocytes restricted to the same immunodominant VP2 epitope in C57BL/6 mice. J Virol 1997;71:5361–5. [PubMed: 9188606]

Feltkamp MC, Vierboom MP, Kast WM, Melief CJ. Efficient MHC class I-peptide binding is required but does not ensure MHC class I-restricted immunogenicity. Mol Immunol 1994;31:1391–401. [PubMed: 7823965]

Feltkamp MC, Vierboom MP, Toes RE, Ossendorp F, ter Schegget J, Melief CJ, Kast WM. Competition inhibition of cytotoxic T-lymphocyte (CTL) lysis, a more sensitive method to identify candidate CTL epitopes than induction of antibody-detected MHC class I stabilization. Immunol Lett 1995;47:1–8. [PubMed: 8537084]

Feuer R, Mena I, Pagarigan R, Slifka MK, Whitton JL. Cell cycle status affects coxsackievirus replication, persistence, and reactivation in vitro. J Virol 2002;76:4430–40. [PubMed: 11932410]

Fuller AC, Kang B, Kang HK, Yahikozowa H, Dal Canto MC, Kim BS. Gender bias in Theiler's virus-induced demyelinating disease correlates with the level of antiviral immune responses. J Immunol 2005;175:3955–63. [PubMed: 16148143]

Goulder PJ, Watkins DI. HIV and SIV CTL escape: implications for vaccine design. Nat Rev Immunol 2004;4:630–40. [PubMed: 15286729]

Granucci F, Foti M, Ricciardi-Castagnoli P. Dendritic cell biology. Adv Immunol 2005;88:193–233. [PubMed: 16227091]

Greter M, Heppner FL, Lemos MP, Odermatt BM, Goebels N, Laufer T, Noelle RJ, Becher B. Dendritic cells permit immune invasion of the CNS in an animal model of multiple sclerosis. Nat Med 2005;11:328–34. [PubMed: 15735653]

Horton H, Russell N, Moore E, Frank I, Baydo R, Havenar-Daughton C, Lee D, Deers M, Hudgens M, Weinhold K, McElrath MJ. Correlation between interferon-γ secretion and cytotoxicity, in virus-specific memory T cells. J Infect Dis 2004;190:1692–6. [PubMed: 15478077]

Hou W, Wu Y, Sun S, Shi M, Sun Y, Yang C, Pei G, Gu Y, Zhong C, Sun B. Pertussis toxin enhances Th1 responses by stimulation of dendritic cells. J Immunol 2003;170:1728–36. [PubMed: 12574336]

Inaba K, Inaba M, Romani N, Aya H, Deguchi M, Ikehara S, Muramatsu S, Steinman RM. Generation of large numbers of dendritic cells from mouse bone marrow cultures supplemented with granulocyte/macrophage colony-stimulating factor. J Exp Med 1992;176:1693–702. [PubMed: 1460426]

Johnson AJ, Njenga MK, Hansen MJ, Kuhns ST, Chen L, Rodriguez M, Pease LR. Prevalent class I-restricted T-cell response to the Theiler's virus epitope D^b:$VP2_{121-130}$ in the absence of endogenous CD4 help, tumor necrosis factor alpha, gamma interferon, perforin, or costimulation through CD28. J Virol 1999;73:3702–8. [PubMed: 10196262]

Kang B, Kang HK, Kim BS. Identification of capsid epitopes of Theiler's virus recognized by CNS-infiltrating $CD4^+$ T cells from virus-infected C57BL/6 mice. Virus Res 2005;108:57–61. [PubMed: 15681055]

Kang BS, Lyman MA, Kim BS. Differences in avidity and epitope recognition of $CD8^+$ T cells infiltrating the central nervous systems of SJL/J mice infected with BeAn and DA strains of Theiler's murine encephalomyelitis virus. J Virol 2002a;76:11780–4. [PubMed: 12388742]

Kang BS, Lyman MA, Kim BS. The majority of infiltrating $CD8^+$ T cells in the central nervous system of susceptible SJL/J mice infected with Theiler's virus are virus specific and fully functional. J Virol 2002b;76:6577–85. [PubMed: 12050370]

Kang BS, Palma JP, Lyman MA, Dal Canto M, Kim BS. Antibody response is required for protection from Theiler's virus-induced encephalitis in C57BL/6 mice in the absence of $CD8^+$ T cells. Virology 2005;340:84–94. [PubMed: 16039687]

Kim BS, Palma JP, Inoue A, Koh CS. Pathogenic immunity in Theiler's virus-induced demyelinating disease: a viral model for multiple sclerosis. Arch Immunol Ther Exp 2000;48:373–9.

Kim KS, Tracy S, Tapprich W, Bailey J, Lee CK, Kim K, Barry WH, Chapman NM. 5'-Terminal deletions occur in coxsackievirus B3 during replication in murine hearts and cardiac myocyte cultures and correlate with encapsidation of negative-strand viral RNA. J Virol 2005;79:7024–41. [PubMed: 15890942]

Lin X, Njenga MK, Johnson AJ, Pavelko KD, David CS, Pease LR, Rodriguez M. Transgenic expression of Theiler's murine encephalomyelitis virus genes in H-2^b mice inhibits resistance to virus-induced demyelination. J Virol 2002;76:7799–811. [PubMed: 12097592]

Lipton HL, Kumar AS, Trottier M. Theiler's virus persistence in the central nervous system of mice is associated with continuous viral replication and a difference in outcome of infection of infiltrating macrophages versus oligodendrocytes. Virus Res 2005;111:214–23. [PubMed: 15893838]

Liuzzi GM, Riccio P, Dal Canto MC. Release of myelin basic protein-degrading proteolytic activity from microglia and macrophages after infection with Theiler's murine encephalomyelitis virus: comparison between susceptible and resistant mice. J Neuroimmunol 1995;62:91–102. [PubMed: 7499498]

Ljunggren HG, Stam NJ, Ohlen C, Neefjes JJ, Hoglund P, Heemels MT, Bastin J, Schumacher TN, Townsend A, Karre K, et al. Empty MHC class I molecules come out in the cold. Nature 1990;346:476–80. [PubMed: 2198471]

Lyman MA, Lee HG, Kang BS, Kang HK, Kim BS. Capsid-specific cytotoxic T lymphocytes recognize three distinct H-$2D^b$-restricted regions of the BeAn strain of Theiler's virus and exhibit different cytokine profiles. J Virol 2002;76:3125–34. [PubMed: 11884537]

Lyman MA, Myoung J, Mohindru M, Kim BS. Quantitative, not qualitative, differences in $CD8^+$ T cell responses to Theiler's murine encephalomyelitis virus between resistant C57BL/6 and susceptible SJL/J mice. Eur J Immunol 2004;34:2730–9. [PubMed: 15368289]

McMahon EJ, Bailey SL, Castenada CV, Waldner H, Miller SD. Epitope spreading initiates in the CNS in two mouse models of multiple sclerosis. Nat Med 2005;11:335–9. [PubMed: 15735651]

Mena I, Roussarie JP, Brahic M. Infection of macrophage primary cultures by persistent and nonpersistent strains of Theiler's virus: role of capsid and noncapsid viral determinants. J Virol 2004;78:13356–61. [PubMed: 15542687]

Mendez-Fernandez YV, Johnson AJ, Rodriguez M, Pease LR. Clearance of Theiler's virus infection depends on the ability to generate a $CD8^+$ T cell response against a single immunodominant viral peptide. Eur J Immunol 2003;33:2501–10. [PubMed: 12938226]

Murray PD, McGavern DB, Lin X, Njenga MK, Leibowitz J, Pease LR, Rodriguez M. Perforin-dependent neurologic injury in a viral model of multiple sclerosis. J Neurosci 1998;18:7306–14. [PubMed: 9736651]

Njenga MK, Pavelko KD, Baisch J, Lin X, David C, Leibowitz J, Rodriguez M. Theiler's virus persistence and demyelination in major histocompatibility complex class II-deficient mice. J Virol 1996;70:1729–37. [PubMed: 8627694]

Palma JP, Lee HG, Mohindru M, Kang BS, Dal Canto M, Miller SD, Kim BS. Enhanced susceptibility to Theiler's virus-induced demyelinating disease in perforin-deficient mice. J Neuroimmunol 2001;116:125–35. [PubMed: 11438167]

Palma JP, Yauch RL, Kang HK, Lee HG, Kim BS. Preferential induction of IL-10 in APC correlates with a switch from Th1 to Th2 response following infection with a low pathogenic variant of Theiler's virus. J Immunol 2002;168:4221–30. [PubMed: 11937584]

Pevear DC, Calenoff M, Rozhon E, Lipton HL. Analysis of the complete nucleotide sequence of the picornavirus Theiler's murine encephalomyelitis virus indicates that it is closely related to cardioviruses. J Virol 1987;61:1507–1516. [PubMed: 3033278]

Pircher H, Moskophidis D, Rohrer U, Burki K, Hengartner H, Zinkernagel RM. Viral escape by selection of cytotoxic T cell-resistant virus variants in vivo. Nature 1990;346:629–33. [PubMed: 1696684]

Pullen LC, Miller SD, Dal Canto MC, Kim BS. Class I-deficient resistant mice intracerebrally inoculated with Theiler's virus show an increased T cell response to viral antigens and susceptibility to demyelination. Eur J Immunol 1993;23:2287–93. [PubMed: 8370406]

Rammensee HG, Friede T, Stevanoviic S. MHC ligands and peptide motifs: first listing. Immunogenetics 1995;41:178–228. [PubMed: 7890324]

Rivera-Quinones C, McGavern D, Schmelzer JD, Hunter SF, Low PA, Rodriguez M. Absence of neurological deficits following extensive demyelination in a class I-deficient murine model of multiple sclerosis. Nat Med 1998;4:187–93. [PubMed: 9461192]

Rossi CP, Delcroix M, Huitinga I, McAllister A, van Rooijen N, Claassen E, Brahic M. Role of macrophages during Theiler's virus infection. J Virol 1997;71:3336–40. [PubMed: 9060706]

Shah AH, Lipton HL. Low-neurovirulence Theiler's viruses use sialic acid moieties on N-linked oligosaccharide structures for attachment. Virology 2002;304:443–50. [PubMed: 12504583]

Velloso LM, Michaelsson J, Ljunggren HG, Schneider G, Achour A. Determination of structural principles underlying three different modes of lymphocytic choriomeningitis virus escape from CTL recognition. J Immunol 2004;172:5504–11. [PubMed: 15100292]

Zhou L, Lin X, Green TJ, Lipton HL, Luo M. Role of sialyloligosaccharide binding in Theiler's virus persistence. J Virol 1997;71:9701–12. [PubMed: 9371636]

Zhou L, Luo Y, Wu Y, Tsao J, Luo M. Sialylation of the host receptor may modulate entry of demyelinating persistent Theiler's virus. J Virol 2000;74:1477–85. [PubMed: 10627559]

Abbreviations

MS

Multiple sclerosis

CNS

central nervous system

TMEV

Theiler's murine encephalomyelitis virus

TMEV-IDD

TMEV-induced demyelinating disease
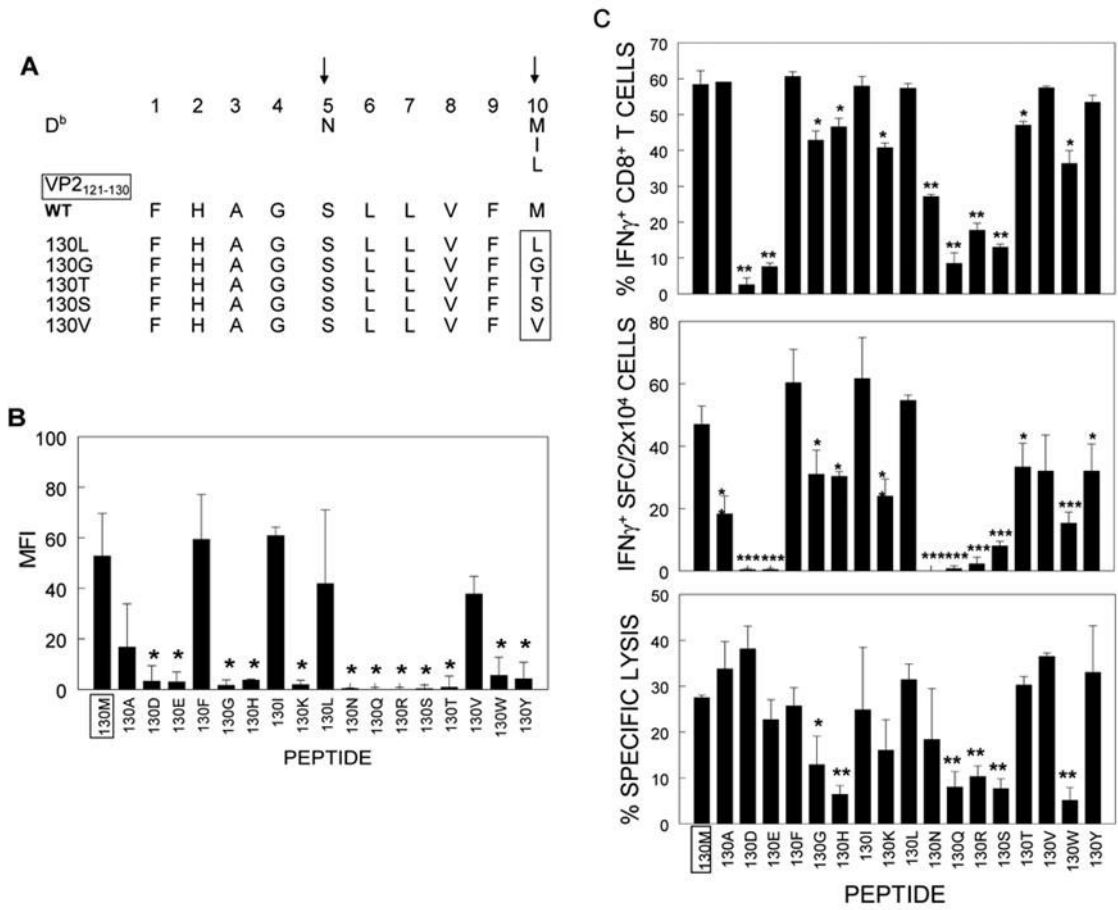
LCMV

lymphocytic choriomeningitis virus

Figure 1. Sequence and binding affinity of peptides with a single amino acid change at VP2$_{130}$ residue within the immunodominant epitope (VP2$_{121-130}$) in C57BL/6 mice

(**A**). The conserved binding motif of H-2D^b molecule and consensus MHC-binding anchor residues (arrows) at positions 5 and 10 (Rammensee, Friede, and Stevanoviic, 1995) are shown. Representative peptide sequences, which contain some substitutions of native residue (M) at the 10th position of VP2$_{121-130}$ epitope are shown and the changed residue is marked by a rectangle. (**B**). The peptides, substituted at the anchor position, were used to assess their binding properties towards H-2D^b. Surface expression of H-2D^b on RMA-S cells was examined by flow cytometric analysis. The level of surface MHC class I molecules is expressed as median fluorescence intensity (MFI) (mean ± SD). The average of 3 independent experiments is shown. (**C**). Immunological reactivity of peptides on CNS-infiltrating CD8$^+$ T cells from infected C57BL/6 mice at 8d post-infection. Intracellular IFN-γ expression in response to peptides was assessed by flow cytometry. IFN-γ-secreting CD8$^+$ T cells in 2×10^4 CNS infiltrates were enumerated by ELISPOT after incubation with each peptide and irradiated 1×10^6 splenic cells as antigen presenting cells. Specific lysis of EL4 cells, loaded with each peptide, by CNS MNC was analyzed in a standard ^{51}Cr release assay (E:T=100:1). IFN-γ ICS, ELISPOT and CTL assays were performed with aliquots of the identical pooled CNS-infiltrating mononuclear cell suspension. Values given for individual panels are the mean of percentage or spots of two to three separate experiments with background subtracted (mean ± SD). *, $p<0.05$; **, $p<0.005$; ***, $p<0.001$ (Student's t test).
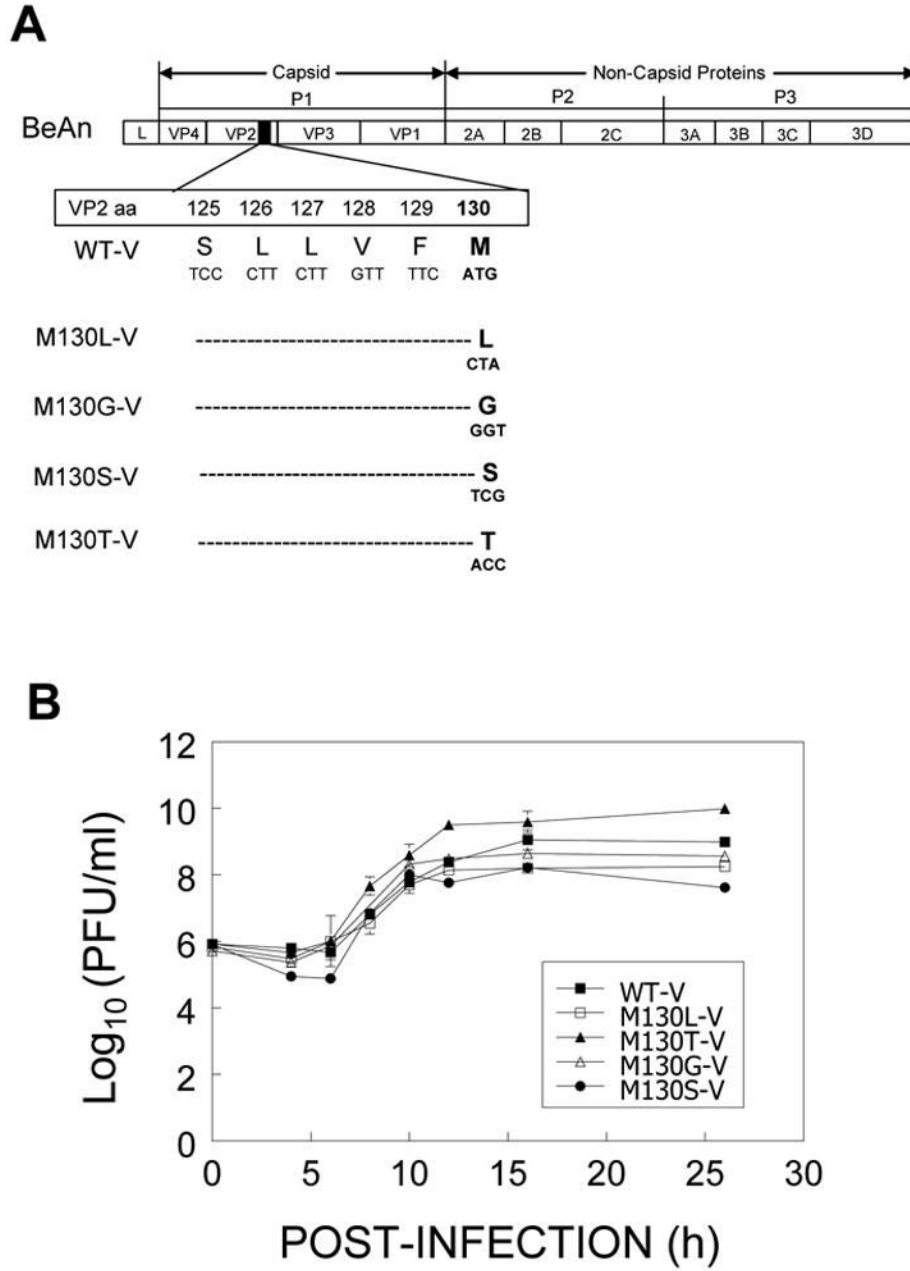
Figure 2. Replication of wild-type and mutant viruses containing a single amino acid substitution at VP2$_{130}$ in BHK 21 cells
A, Schematic diagram of site-directed mutagenesis of TMEV BeAn strain. Amino acid and DNA sequences of wild-type and selected mutant viruses are presented. **B**, *In vitro* growth of wild-type and mutant viruses in BHK cells. Viruses recovered from the cultures at the indicated time point were assayed for viral replication by plaque assay. Viral titer is expressed as log10 PFU/ml (mean of triplicates ± SEM).
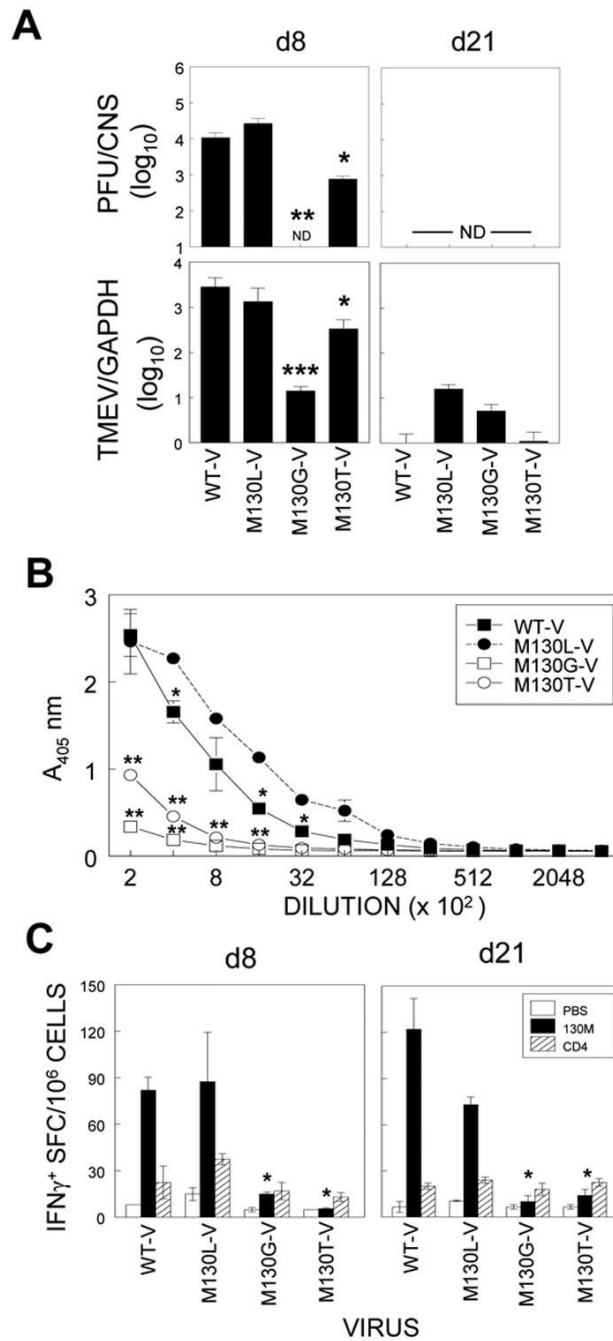
Figure 3. Comparison of viral persistence and peripheral immune responses in WT or mutant virus-infected mice

A, Viral load in the CNS (pooled brains and spinal cords from at least three mice per group) of C57BL/6 mice infected with indicated viruses was determined by plaque assay at 8 and 21 days post-infection. M130L-V-infected mice showed comparable viral load to wild-type virus at day 8 post-infection while the level of recovered virus from M130G-V and M130T-V-infected mice was significantly lower than those from M130L-V or WT-V infected mice. (*, $p<0.05$; **, $p<0.001$). The detection limit for infectious viral titres in the brain or spinal cord was 50 PFU. Detection limit of plaque assay was <50 PFU/CNS. Viral levels bellow detectable by plaque assay, were indicated as not detectable (ND). Real-time PCR of cDNAs from the

CNS of mice infected with WT and variant TMEV for 8 and 21 days was performed with specific primers. Data are expressed as means ± SD for triplicate determinations. *, $p<0.05$; **, $p<0.005$; ***, $p<0.001$ (Student's t test).

B, TMEV-specific IgG response was analyzed by ELISA. Pooled sera from 3 mice infected with the indicated virus were used for the assessment. The level of virus-specific IgG in the sera of M130G-V and M130T-V-infected mice was significantly lower compared to that of M130L-V and WT-infected animals ($p<0.05$). **C**, Epitope-specific $CD8^+$ and $CD4^+$ T cell responses were assessed by ELISPOT assay. Spleen cells (1×10^6) from 3 mice infected with the indicated virus were incubated in the presence of $VP2_{121-130}$ or a mixture of $CD4^+$ T cell epitopes ($VP4_{25-38}$ and $VP2_{206-220}$) for 16 to 18 h. M130G/T-V induced significantly lower number of epitope-specific $CD8^+$ T cells in the spleen compared to WT-V (*, $p<0.05$; **, $p<0.001$).
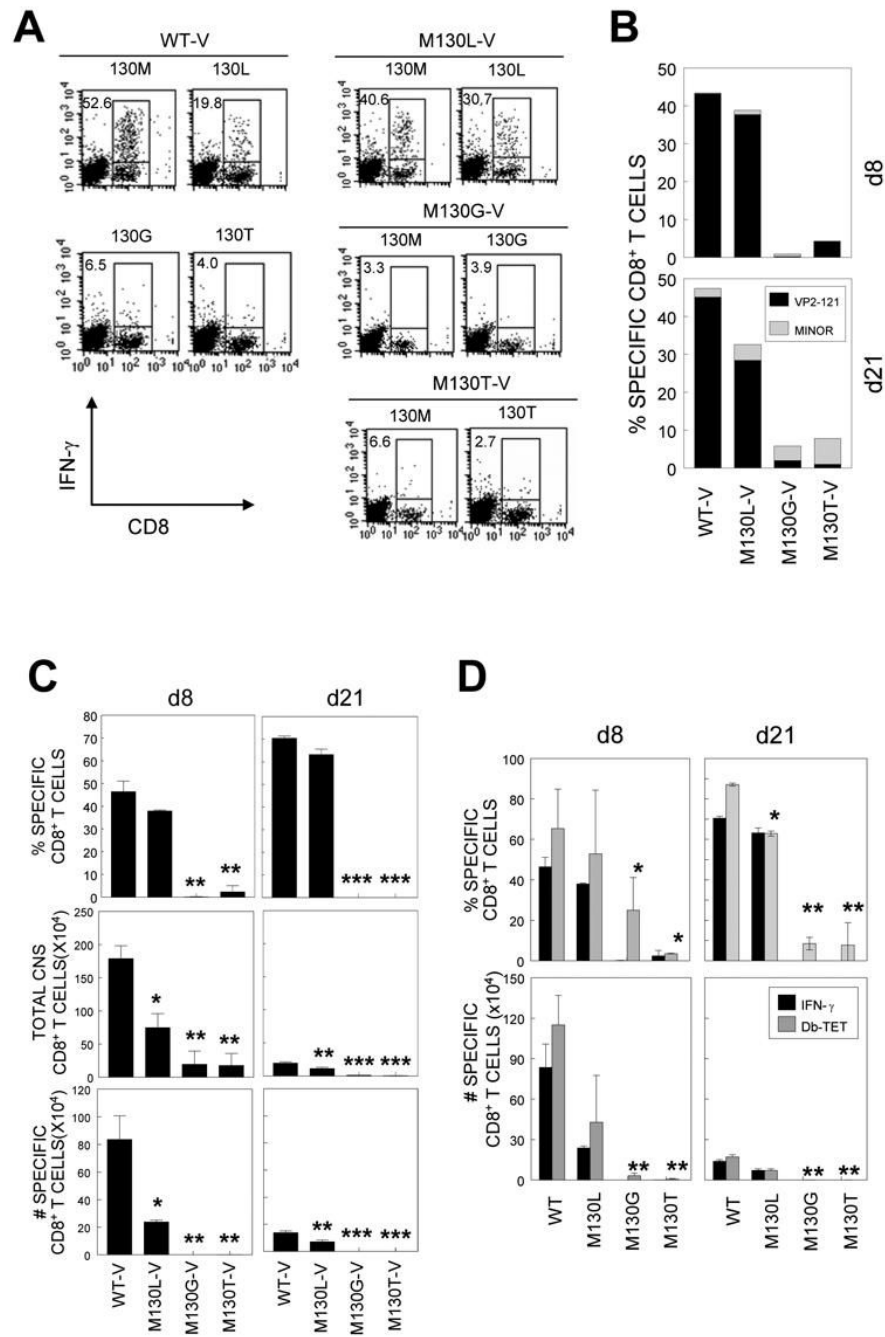
Figure 4. Epitope-specific IFN-γ-producing CD8⁺ T cell in the CNS of WT or mutant virus-infected mice

A, CNS-infiltrating cells were stimulated with indicated peptides at 2 μM for 6 h. Cells were stained for both CD8 and intracellular IFN-γ followed by flow cytometric analysis. The percentage of IFN-γ⁺CD8⁺ T cells is shown in the upper left quadrant of each plot. Data are representative of 3 independent experiments. **B**, CNS-infiltrating cells from mice at 8 d and 21 d post infection were stimulated with the predominant (VP2$_{121–130}$) or a mixture of minor epitope peptides (VP2$_{165–173}$ and VP3$_{110–120}$) for 6 h and the percentage of IFN-γ⁺CD8⁺ T cells was determined. **C**, Proportion of epitope-specific CD8⁺ T cells (Top panel), total number of CNS-infiltrating MNC (middle panel), and the number of epitope-specific CD8⁺ T cells in

the CNS (bottom panel) is shown. Values given are the mean of percentage or numbers of at least two independent experiments (mean ± SD). **D**, Comparison of D^b-VP2$_{121-130}$ tetramer-positive and VP2$_{121-130}$-specific IFN-γ-positive CNS-infiltrating CD8$^+$ T cells. CNS-infiltration of specific CD8$^+$ T cells in mice infected with M130G-V and M130T-V was significantly lower compared to that in mice infected with WT-V or M130L-V. *, $p<0.05$; **, $p<0.01$.
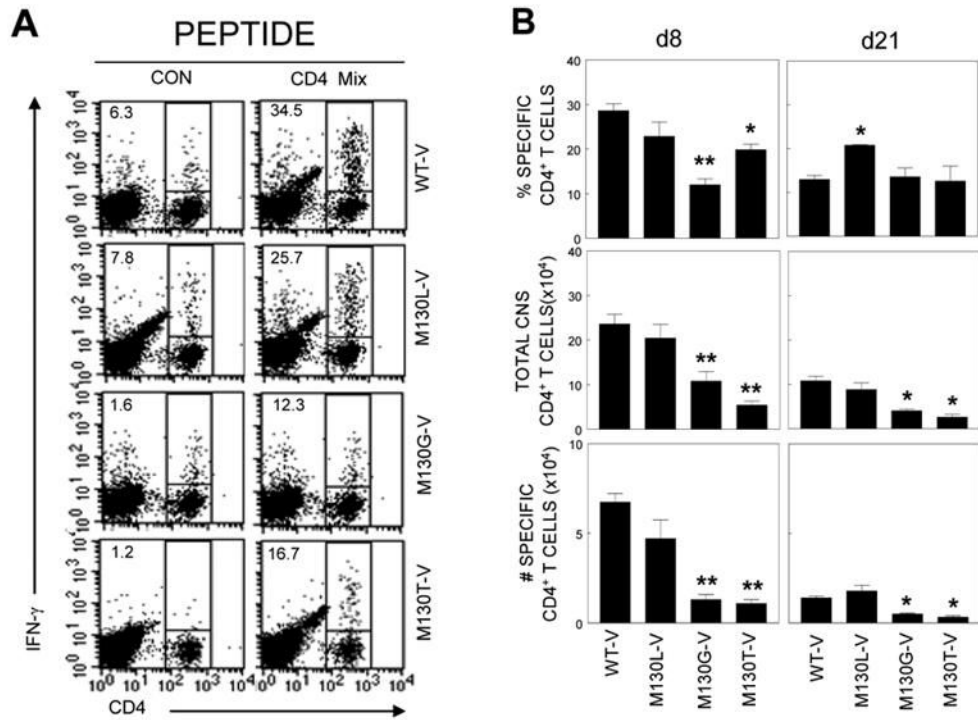
Figure 5. Epitope-specific IFN-γ-producing CD4⁺ T cells in the CNS of WT or mutant virus-infected mice
A, Isolated CNS-infiltrating MNC were re-stimulated with a mixture of CD4⁺ T cell-specific epitopes (VP2$_{206-220}$ and VP4$_{25-38}$) for 6 hours. Cells were stained for CD4 and intracellular IFN-γ. The percentage of CD4⁺ and IFN-γ⁺ cells is shown on the upper left corner of each plot. Data are representative of 3 independent experiments. **B**, Histograms represent the mean of percentage or numbers of 2–3 independent experiments by FACS analysis. Proportion of epitope-specific CD4⁺ T cells (Top panel), total number of CNS-infiltrating CD4⁺ T cells (middle panel), and the number of epitope-specific CD4⁺ T cells in the CNS (bottom panel) is shown.
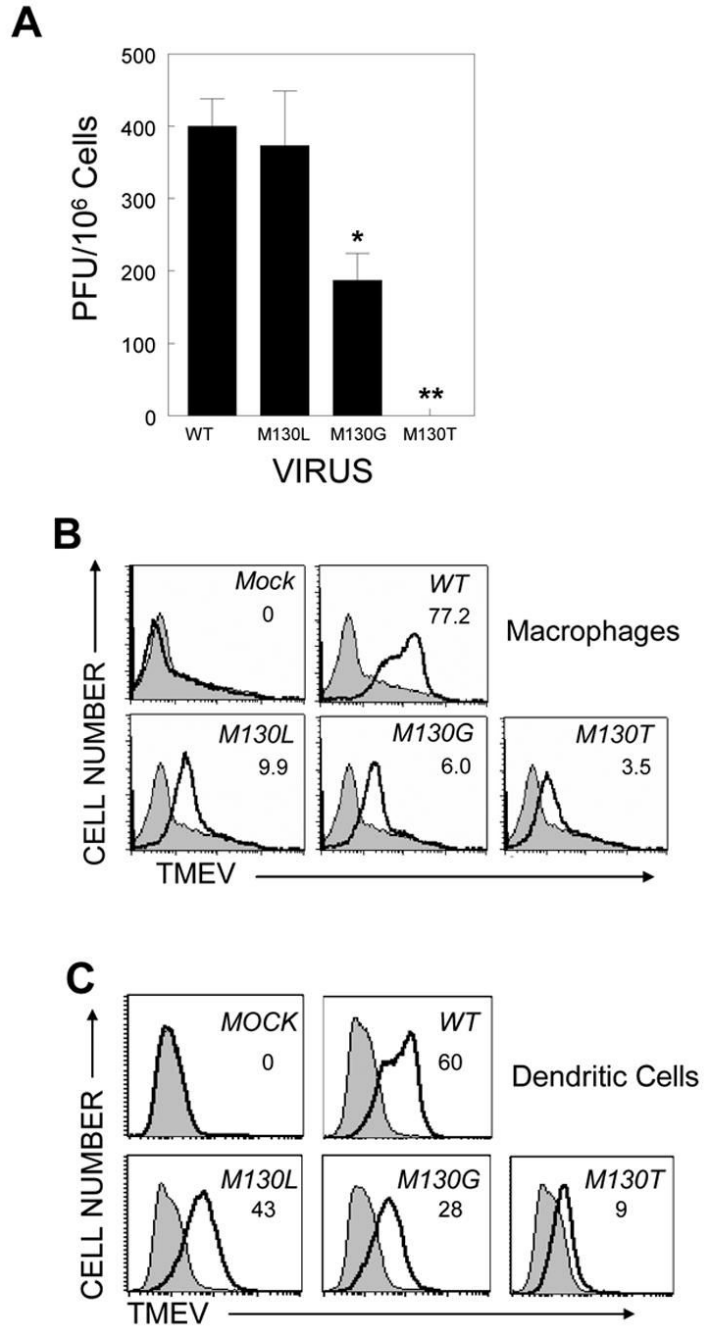
Figure 6. Viral replication in primary macrophages and binding to primary cells derived from C57BL/6 mice
A, Primary macrophages were infected with each virus and the cell culture supernatant was assessed for virus titres by plaque assay. Values given represent the number of plaques per 10^6 peritoneal macrophages (mean ± SD). Statistical analysis was performed by Student's *t* test. *, $p<0.05$; **, $p<0.005$. Viral binding to macrophages (**B**) or DC (**C**) derived from C57BL/ 6 mice was assessed. In all plots, filled histograms and open histograms represent staining with an isotype control Ab and monoclonal Ab specific to TMEV, respectively. Numbers in each histogram plot indicate subtracted MFI value (MFI with TMEV-specific antibody – MFI with control Ab).